Dependence of Heavy-ion Fusion Reaction on Nuclear Deformation and Nuclear Shell Structure

H. Ikezoe,* **S. Mitsuoka, K. Nishio, K. Satou, and I. Nishinaka**

Advanced Science Research Center, Japan Atomic Energy Research Institute, Tokai, Ibaraki 319-1195, Japan

The dependence of the fusion probability on the orientation of deformed nucleus was investigated for the reactions ^{60,64}Ni + ^{154}Sm and ^{76}Ge + ^{150}Nd. Evaporation residues were measured for these reaction systems by the JAERI recoil mass separator in the vicinity of the Coulomb barrier and the fusion probability was extracted as a function of bombarding energy. It was found that the fusion probability depends strongly on the orientation of the nuclear deformation. The fusion probability is considerably reduced when the projectiles collide at the tip of the deformed nuclei. On the other hand, when the projectiles collide at the side of the deformed nuclei, the fusion occurs without hindrance. This phenomenon is understood qualitatively by comparing the distance between the mass centers of two colliding nuclei at touching with the position of the saddle point of the compound nucleus. The dependence of the fusion probability on the nuclear shell closure was also investigated for the reactions ^{82}Se + ^{134,138}Ba, where the nucleus ^{138}Ba has a closed neutron shell of $N = 82$ and the nucleus ^{134}Ba has the neutron number $N = 78$, four neutrons less than the closed shell. The measured evaporation residue cross section for the reaction ^{82}Se + ^{138}Ba was well reproduced by statistical model calculations taking into account a subbarrier fusion enhancement, while the evaporation residue cross section for the reaction ^{82}Se + ^{134}Ba was about 100 times smaller than that for the fusion reaction ^{82}Se + ^{138}Ba. This suggests that the shell closure plays an important role in the fusion process.

1. Introduction

Heavy-ion fusion reaction between massive nuclei has been extensively investigated so far. It is well known that the fusion probability between massive nuclei depends on the charge product $Z_p Z_t$ of projectile and target.[1] When the charge product is larger than about 1800, the fusion probability decreases rapidly as $Z_p Z_t$ increases. This means that even if the kinetic energy of projectile is large enough to surmount the fusion barrier, a compound nucleus is not always formed. An additional kinetic energy is needed to form the compound nucleus. The compound nucleus is formed after the saddle point of the compound nucleus is passed through in the course of the fusion process after touching. A large kinetic energy is lost during this process. This means that the compact touching shape evolves more easily into the compound nucleus than an elongated touching shape. Thus the relative distance between the mass center of two colliding nuclei at touching with respect to the saddle point plays an essential role for fusion of massive reaction system. The contact point of massive reaction system with a large charge product (>1800) usually located outside the saddle point. This situation is changed in the case of deformed nucleus and spherical projectile, because the distance between the mass centers at touching depends on the orientation of deformed nucleus. This suggests that the fusion process is affected by the colliding angle θ with respect to the symmetric axis of deformed nucleus. This was investigated by measuring evaporation residues (ERs) in the reaction ^{60,64}Ni + ^{154}Sm and ^{76}Ge + ^{150}Nd, where the nuclei ^{154}Sm and ^{150}Nd are well deformed.

The fusion between massive nuclei depends on not only the charge product but also the nuclear structure of projectile and target. It is reported that the number of valence nucleon outside a major shell affects the fusion probability.[1] Recently, Oganessian et al.[2] measured the evaporation residues in the fusion reactions ^{130}Xe + ^{86}Kr and ^{136}Xe + ^{86}Kr, where the nuclei ^{136}Xe and ^{86}Kr have the closed neutron shells $N = 82$ and $N = 50$, respectively, and the nucleus ^{130}Xe has no such a closed shell. They found that the measured evaporation residue cross sections for the fusion reaction ^{136}Xe + ^{86}Kr are almost 2 ∼ 3 orders of magnitude

larger than those for the fusion reaction ^{130}Xe + ^{86}Kr. This suggests the important role of the shell closure of the colliding nuclei in the fusion process. In this paper, we report the results of the ERs measurements for the two reactions ^{82}Se + ^{134}Ba and ^{82}Se + ^{138}Ba, where the nucleus ^{138}Ba has the neutron shell closure $N = 82$ and the nucleus ^{134}Ba has the neutron number 78, four neutrons less than the closed shell.
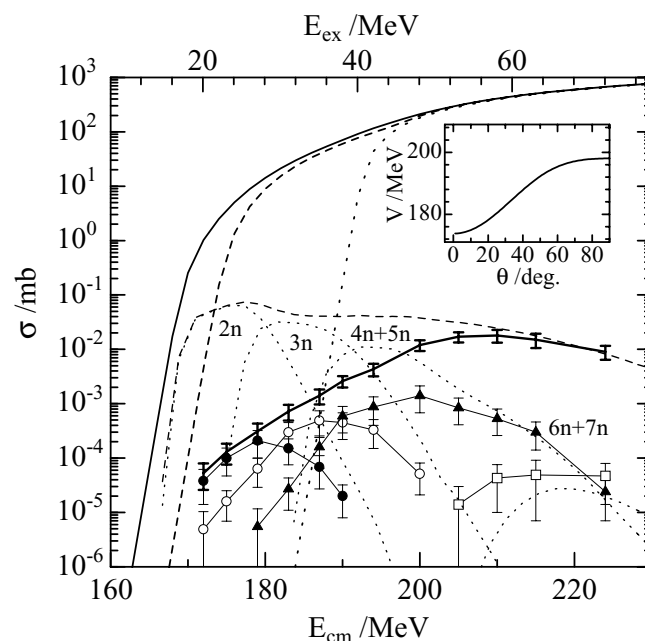
Figure 1. Measured evaporation residue cross sections of the *xn* channels for the reaction ^{64}Ni + ^{154}Sm as a function of the center-of-mass energy E_{cm} and also the excitation energy E_{ex} of the compound nucleus. Each channel for the evaporation is shown as the solid circles (2*n*), open circles (3*n*), solid triangles (4*n* + 5*n*), and open squares (6*n* + 7*n*). The total cross section of the measured ERs is shown as the thick solid curve with error bar. The thin dotted and the thin dashed curves are the calculated cross sections of the *xn* evaporation residues and the sum of the ERs, respectively. The fusion cross sections are calculated by taking into account the deformation of ^{154}Sm together with the 2^+ and 3^- excitations (the solid curve), only the deformation (the long dashed curve), and without the deformation (the dotted curve). The fusion barrier *V* is shown as a function of the colliding angle θ in the inset.

*Corresponding author. E-mail: ikezoe@popsvr.tokai.jaeri.go.jp.
FAX: +81-29-282-5927.

2. Experimental Results and Discussion

2.1. Deformation Effect. We measured the ERs for the reactions ^{60,64}Ni + ^{154}Sm ($Z_pZ_t = 1736$)[3] and ^{76}Ge + ^{150}Nd ($Z_pZ_t = 1920$)[4] by using the JAERI recoil mass separator.[5] The experimental details are described elsewhere.[3,4] Figure 1 shows the *xn*-channel cross sections of the ERs for the fusion reaction ^{64}Ni + ^{154}Sm. The total cross section of the measured ERs is also shown. The nucleus ^{154}Sm has a large β_2 deformation of 0.32. This gives rise to a broad barrier distribution *V* as shown in the inset of Figure 1 and thus the fusion cross section (the solid curve) is enhanced below the Bass barrier 192.8 MeV. The standard statistical model calculation (HIVAP),[6] combined with the calculated fusion cross sections by using the code CCDEF,[7] predicts the sizable cross sections for the 2*n* and 3*n* channels (the thin dotted curves) below the Bass barrier. The reason is as follows: when the spherical ^{64}Ni projectile collides at the tip part ($\theta < 40°$) of the prolate ^{154}Sm nucleus, where the fusion barrier is the lowest about 180 MeV as shown in the inset of Figure 1, a low excited compound nucleus of about 30 MeV is formed. This compound nucleus emits two or three neutrons in the de-excitation process. This means that the residues produced in the 2*n* and 3*n* channels are expected only at the energies below the Bass barrier and thus these cross sections are very sensitive to the fusion probability at these energies, that is, at the tip collision.
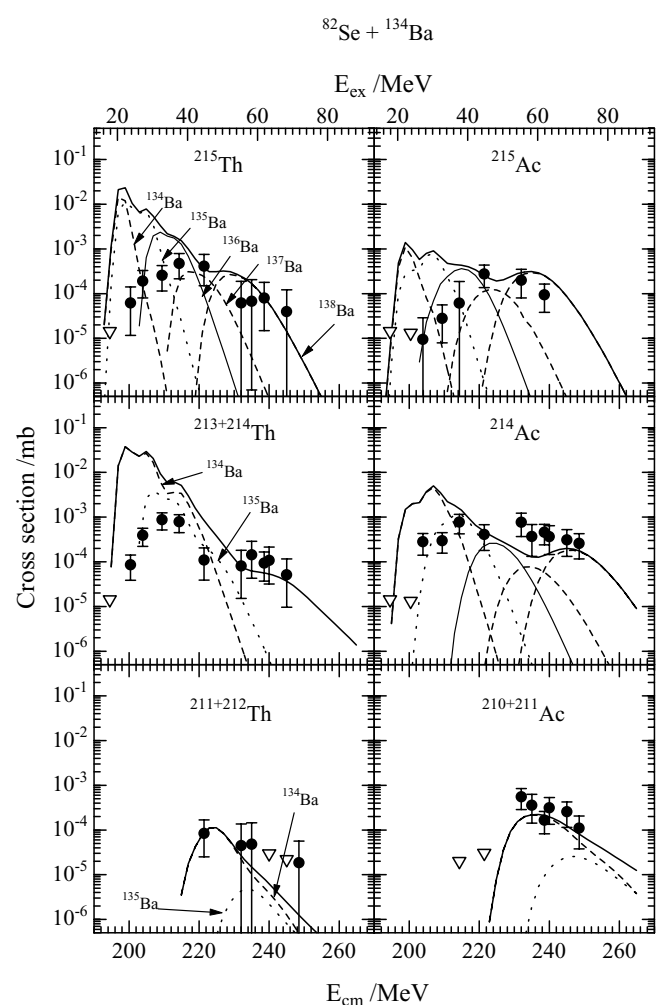
The measured cross sections for these channels were considerably smaller than the predictions. The total cross section of the measured ERs including the residues of Th, Ac, and Ra also deviates from the calculated result (the thin dashed curve) below 200 MeV and then increases gradually to the calculated values as the center-of-mass energy E_{cm}. This means that the actual fusion barrier at the tip collision is effectively larger than the calculation shown in the inset of Figure 1. In other words, an extra-push energy is needed to push a di-nuclear system formed at the tip collision into the formation of the compound nucleus. As for the side collision ($\theta > 70°$), the present data show that the fusion occurs without hindrance, because the predicted cross sections for the 4*n* + 5*n* and 6*n* + 7*n* channels and also the total ERs cross section at $E_{cm} > 200$ MeV are consistent with the measured data. We obtained the same conclusion as mentioned here in the fusion reactions ^{60}Ni + ^{154}Sm (Ref. 3) and ^{76}Ge + ^{160}Nd (Ref. 4).

The present results can be qualitatively understood by considering the position of the contact point relative to the saddle point of the compound nucleus. In the case of the reaction system ^{64}Ni + ^{154}Sm, the minimum distance $R_{min}/R_0 = 1.48$ between the mass centers corresponds to the side collision and is close to the position of the saddle point $R_{saddle}/R_0 \sim 1.5$ of the compound nucleus ^{218}Th. Here the position of the saddle point was estimated from Reference 8. R_0 is the radius of the compound nucleus. On the other hand, the maximum distance $R_{max}/R_0 = 1.77$ corresponding to the tip collision is well outside the saddle point. In the case of the reaction system ^{76}Ge + ^{150}Nd, the maximum distance of 1.76 corresponding to the tip collision
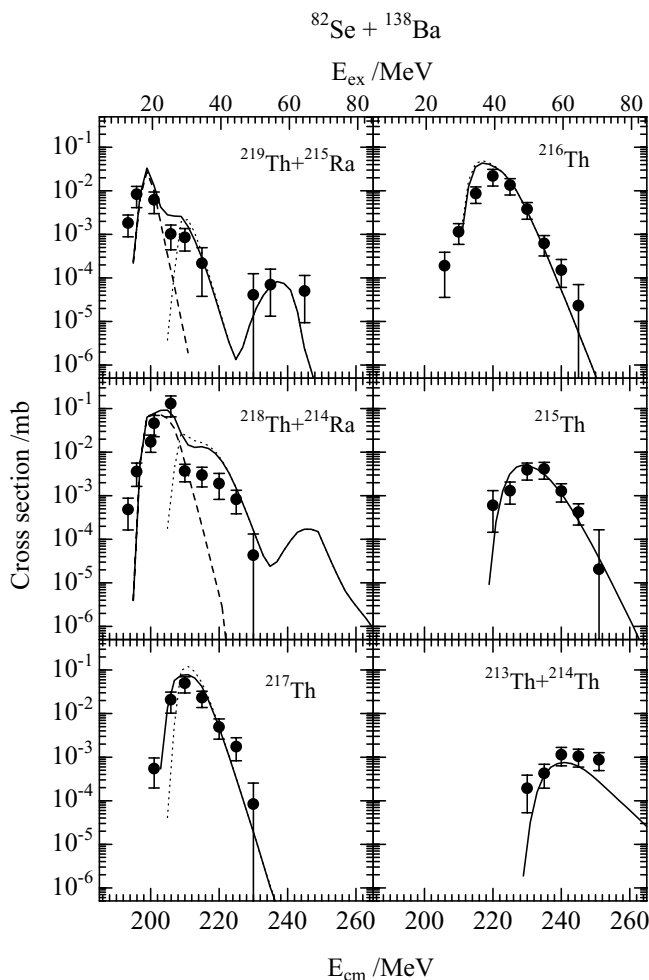
Figure 2. Measured evaporation residue cross sections for the reaction ^{82}Se + ^{138}Ba. The measured residues are indicated in each figure. The calculated cross sections of the *xn* evaporation residues are shown as the solid curves and especially the calculated 1*n* and 2*n* channel cross sections are shown as the dashed curves in upper left figures. In this calculation, the coupling of the inelastic excitations of the first 2$^+$ and 3$^-$ states for both the projectile and the target were taken into account. The calculated results without the coupling of these inelastic excitations are also shown as the dotted curves.

Figure 3. Same as Figure 2 but for the fusion reaction ^{82}Se + ^{134}Ba. The open triangles show the upper limit of the measured cross sections. In this reaction, the contaminations of the barium isotopes 135, 136, 137, and 138 in a ^{134}Ba target were 15.24%, 4.03%, 1.94%, and 5.26%, respectively. The calculated contributions due to these contaminations are shown by the curves pointed by arrows. The cross sections measured above $E_{cm} > 230$ MeV are mainly ascribed to the heavy barium isotopes $A > 135$.
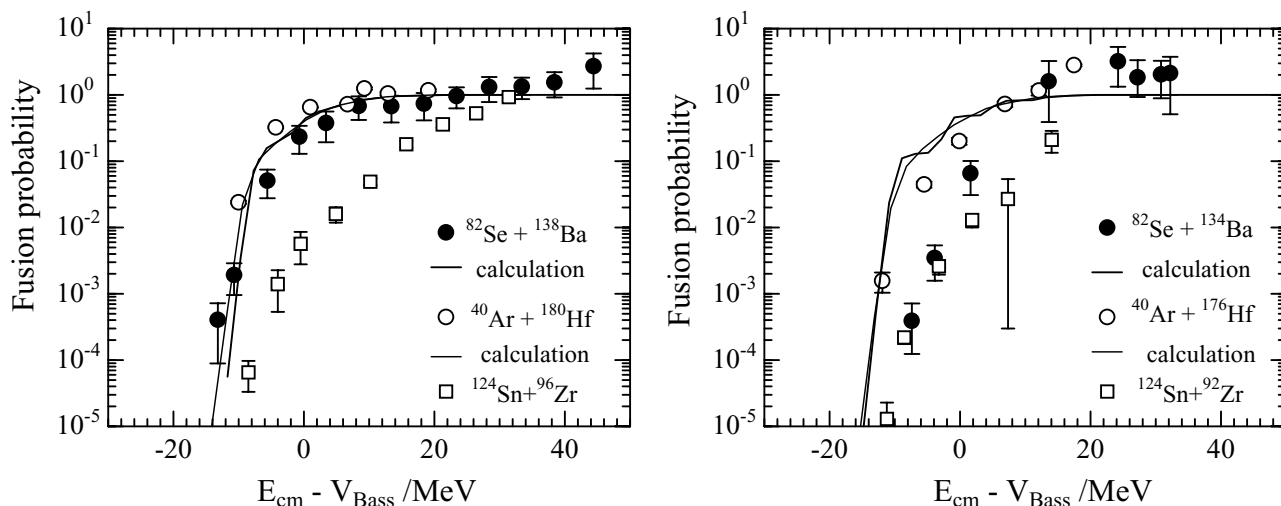
Figure 4. Fusion probability obtained from the measured ERs cross sections for the reactions ^{82}Se + ^{138}Ba (left) and ^{82}Se + ^{134}Ba (right). V_{Bass} shows the Bass barrier. The solid curves show the calculated fusion probabilities without fusion hindrance. The data for the fusion reactions ^{40}Ar + ^{176,180}Hf (Ref. 10) and ^{124}Sn + ^{92,96}Zr (Ref. 6) are also plotted to make a comparison with the present data. Here the three reaction systems shown in the left and the right figures make the same compound nuclei ^{220}Th and ^{216}Th, respectively.

is outside the saddle point $R_{saddle}/R_0 \sim 1.4$ of the compound nucleus ^{226}U. The minimum distance of 1.43 at the side collision is close to the saddle point. Since the compact configuration at the contact point tends to evolve into the formation of the compound nucleus compared with more elongated configuration, the compound nucleus may be more easily formed for the side collisions than the tip collision for the present reaction systems. Although the present results show that the tip collision exhibits a large fusion hindrance, some ERs corresponding to the 2n and 3n channels still exist with small cross sections. This is because of a large survival probability against fission at low excitation energy. On the other hand, the side collision makes the compound nucleus with high excitation because of a high Coulomb barrier. It turns out that the survival probability becomes small at a high excitation energy because of a large fission channel. This is a shortcoming for the side collision.

2.2. Shell Structure Effect. We also investigated the dependence of the fusion probability on the nuclear structure, especially on the neutron closed shell $N = 82$. The evaporation residues in the two fusion reactions ^{82}Se + ^{138}Ba and ^{82}Se + ^{134}Ba were measured. Here the same compound nucleus ^{216}Th is formed for both the fusion reactions ^{82}Se + ^{134}Ba and ^{130}Xe + ^{86}Kr (Ref. 2). The evaporation residues were measured by the similar methods in References 3, 4. The measured evaporation residue cross sections for the fusion reactions ^{82}Se + ^{138}Ba and ^{82}Se + ^{134}Ba are shown in Figure 2 and Figure 3, respectively, together with the statistical model predictions taking into account the barrier distribution due to the coupling of the first 2^+ and 3^- inelastic excitations of target and projectile nuclei. In the fusion reaction ^{82}Se + ^{138}Ba, the maximum cross sections of the 2n and 3n channels are about 0.05 $\sim$ 0.1 mb, while those for the fusion reaction ^{82}Se + ^{134}Ba are $\sim$1 μb. It should be noted that in the 2n + 3n channels for the fusion reaction ^{82}Se + ^{134}Ba, there are additional contributions from the fusion reactions due to the contamination of heavy barium isotopes $A > 134$ in the ^{134}Ba target (see the figure caption of Figure 3).

The excellent agreement between the measured ERs cross sections and the calculated results in the reaction system ^{82}Se + ^{138}Ba means that there is no fusion hindrance. On the other hand, there are large deficits in the xn channel cross sections for the fusion reaction ^{82}Se + ^{134}Ba at the low energy region ($E_{ex} < 40$ MeV) compared with the statistical model predictions. Figure 4 shows the fusion probability obtained from the sum of the ERs cross sections including xn and pxn channels. The fusion probability for the reaction system ^{82}Se + ^{134}Ba was obtained by subtracting the other contribution ascribed to the heavy barium isotopes in the target. As shown in Figure 4, the

fusion probability for the reaction system ^{82}Se + ^{134}Ba is smaller than the prediction near the barrier region, which shows the similar trend with the more symmetric reaction system ^{124}Sn + ^{92}Zr (Ref. 9). This result indicates a fusion hindrance at the barrier region. On the other hand, the fusion probability for the reaction system ^{82}Se + ^{138}Ba is close to the one for the more asymmetric reaction system ^{40}Ar + ^{180}Hf (Ref. 10) and clearly different from the trend for the fusion probability of the more symmetric reaction system ^{124}Sn + ^{96}Zr. This means no fusion hindrance for the reaction system ^{82}Se + ^{138}Ba.

The present result is consistent with that of the fusion reaction ^{130,136}Xe + ^{86}Kr (Ref. 2). These results indicate the importance of the nuclear shell structure in the sub-barrier fusion. This may be related with the fission of the thorium isotopes as pointed out by Oganessian.[2] The asymmetric fission of thorium isotopes is observed for ^{220}Th and ^{222}Th but not for ^{216}Th (Ref. 2, 11). The both fission fragments at scission of these asymmetric fission are spherical and the atomic number of the heavy asymmetric component is concentrated around $Z_H = 54$ with a small charge width of 4.7 (FWHM).[11] The projectile and target nuclei in reaction system ^{82}Se + ^{138}Ba are close to the asymmetric fission fragments of ^{220}Th and also the colliding partner in the reaction system ^{136}Xe + ^{86}Kr is close to the asymmetric fission fragments of ^{222}Th. The potential energy calculated at touching also shows a minimum for these target-projectile combinations because of large negative shell energies of these projectiles and target nuclei.[12] These target-projectile combination makes a compact touching shape and produces a cold compound nucleus when they fuse. The present result means that the fusion of massive reaction system strongly depends on the nuclear shell structure of colliding partners and the target-projectile combination corresponding to the asymmetric fission product plays an important role in the fusion process. In order to make clear the relation between fusion and fission, further experimental and theoretical investigations are needed.

References

(1) A. B. Quint, W. Reisdorf, K.-H. Schmidt, P. Armbruster, F. P. Hessberger, S. Hofmann, J. Keller, G. Münzenberg, H. Stelzer, H.-G. Clerc, and C.-C. Sahm, Z. Phys. A **346**, 119 (1993).

(2) Yu. Ts. Oganessian, *Heavy Elements and Related New Phenomena*, edited by W. Greiner and R. K. Gupta (World Sci-

entific, Singapore, 1999), p. 43.

(3) S. Mitsuoka, H. Ikezoe, K. Nishio, and J. Lu, Phys. Rev. C **62**, 054603 (2000).

(4) K. Nishio, H. Ikezoe, S. Mitsuoka, and J. Lu, Phys. Rev. C **62**, 014602 (2000).

(5) H. Ikezoe, Y. Nagame, T. Ikuta, S. Hamada, I. Nishinaka, and T. Ohtsuki, Nucl. Instrum. Methods A **376**, 420 (1996).

(6) W. Reisdorf and M. Schädel, Z. Phys. A **343**, 47 (1992).

(7) J. O. Fernández Niello, C. H. Dasso, and S. Landowne, Comput. Phys. Commun. **54**, 409 (1989).

(8) P. Möller and J. R. Nix, Nucl. Phys. A **272**, 502 (1976).

(9) C.-C. Sahm, H.-G. Clerc, K.-H. Schmidt, W. Reisdorf, P. Armbruster, F. P. Hessberger, J. G. Keller, G. Münzenberg, and D. Vermeulen, Nucl. Phys. A **441**, 316 (1985).

(10) H.-G. Clerc, J. G. Keller, C.-C. Sahm, K.-H. Schmidt, H. Schulte, and D. Vermeulen, Nucl. Phys. A **419**, 571 (1984).

(11) K.-H. Schmidt, S. Steinhauser, C. Bockstiegel, A. Grewe, A. Heinz, A. R. Junghans, J. Benlliure, H.-G. Clerc, M. de Jong, J. Muller, M. Pfutzner, and B. Voss, Nucl. Phys. A **665**, 221 (2000).

(12) R. K. Gupta and W. Greiner, *Heavy Elements and Related New Phenomena*, edited by W. Greiner and R. K. Gupta (World Scientific, Singapore, 1999), p. 397.